Proceedings of the SEM Annual Conference
June 7-10, 2010 Indianapolis, Indiana USA

Mechanical Properties Measurement of Sand Grains by Nanoindentation

Fang Wang, Boshen Fu, Reza A. Mirshams[1], William Cooper[2], Ranga Komanduri[3],
Hongbing Lu
Department of Mechanical Engineering
University of Texas at Dallas, Richardson, TX 75080
[1]University of North Texas, Denton, TX 76203
[2]Air Force Research Laboratory, Eglin Air Force Base, FL 32542
[3] Mechanical and Aerospace Engineering, Oklahoma State University, Stillwater, OK 74078
hongbing.lu@utdallas.edu

ABSTRACT

Nanoindentation was conducted on sand grains to measure the Young's modulus, hardness, and fracture toughness of individual sand grains. An inverse problem solving approach was used to determine the stress-strain relationship of sand by allowing finite element simulated load-displacement relationship to agree with measurement data. A cube-corner indenter tip was used to induce cracks emanating from the corners of the indenter tip to measure the fracture toughness. X-Ray Diffraction (XRD) technique was used to determine the crystal structure of sand grains.

1. Introduction

As a granular material, sand is conglomerate of discrete particles held together (but not bonded) with significant void space (50-64%) in between. Mechanical properties of sand grains, such as the Young's modulus, hardness, fracture toughness, and stress-strain relationships are of particular importance since their individual behavior dictates the overall behavior of the sand at macro scale. Moreover, the mechanical properties of the grains can vary with the mineral composition of sand, size, defect structure, and crystal orientation. The effect of grain size is due to the fact that larger grains would contain higher number of defects in the form of voids and ridges as well as cracks which may yield mechanical properties different than the smaller grain sizes. Furthermore, since the smaller sand grains usually stay at top layers and may affect more by wind while larger sand grains usually settles at bottom that may affect more by pressure which may cause different crystal structures and mechanical properties of sand grains with different sizes.

Nanoindentation technique is widely used to extract mechanical properties of small volume of materials. In this investigation, we have carried out nanoindentation tests using a Berkovich indenter on six different size groups of sand grains and recorded the load-displacement data. Young's modulus and hardness were obtained directly from the MTS Testworks software output based on the analysis of unloading segment using the method developed by Oliver and Pharr [1]. The representative stress-strain curves for different size samples were obtained, corresponding to the representative modulus and hardness obtained, for solving an inverse problem to determine the stress-strain relationship using FEM. Cubecorner nanoindenter tip was also used to generate cracks for measurement of fracture toughness. In all the cases the indent impressions were obtained using (MTS) NanoVision module. The lengths of the cracks developed were used to determine the range of fracture toughness values for the sand grains. Statistical analysis was conducted to determine the variability in the mechanical properties of sand grains.

2. Sand sample characterization

A sample of Eglin sand was washed and subsequently dried in an oven. The sample sand used for nanoindentation has widely distributed sizes. Multidirectional shaker was used to determine the size of the sand grains. The sieves use metal wire cloth with A.S.T.M. E-11 standard sieve series. To separate different sizes of the sand, the sand agglomerate is vibrated through a series of progressively smaller sieves that are stacked on

T. Proulx (ed.), *Time Dependent Constitutive Behavior and Fracture/Failure Processes, Volume 3*, Conference Proceedings of the Society for Experimental Mechanics Series 15, DOI 10.1007/978-1-4419-9794-4_19, © The Society for Experimental Mechanics, Inc. 2011

top of one another. After 10 minutes shaking time, the sand that falls through a mesh is given the designation of passed weight and the sand that remains on top of that mesh is designated as remaining weight. The passed weight versus grain size curve was plotted to obtain the sand size distribution curve as shown in Figure 1.

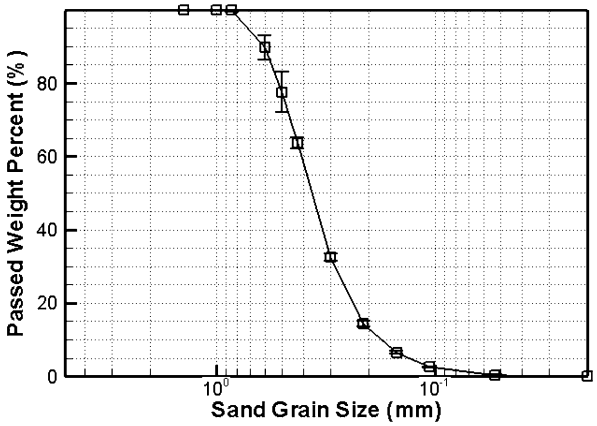

Figure 1. Size distribution curve of sand grains

In order to detect the crystal structure of sand grains, x-ray diffraction (XRD) tests were conducted on sand grains with different sizes. The XRD results were shown in Figure 1. The diffraction patterns of six sizes of sand grain samples are demonstrated in Figure 2 (a). Since the sand grains samples are randomly selected, the intensity values may vary for different batches thus are not given in the figure. Although most of the diffraction peak angles are same, there are some differences between these six patters which indicate sand grains with different sizes may have different crystal structures caused by different material constituents, defect structure etc. Comparing sand diffraction data against the database maintained by the International Centre for Diffraction Data, it is found the 0.212 mm size sand grain pattern can almost fully match the quartz diffraction pattern (Figure 2 (b)).

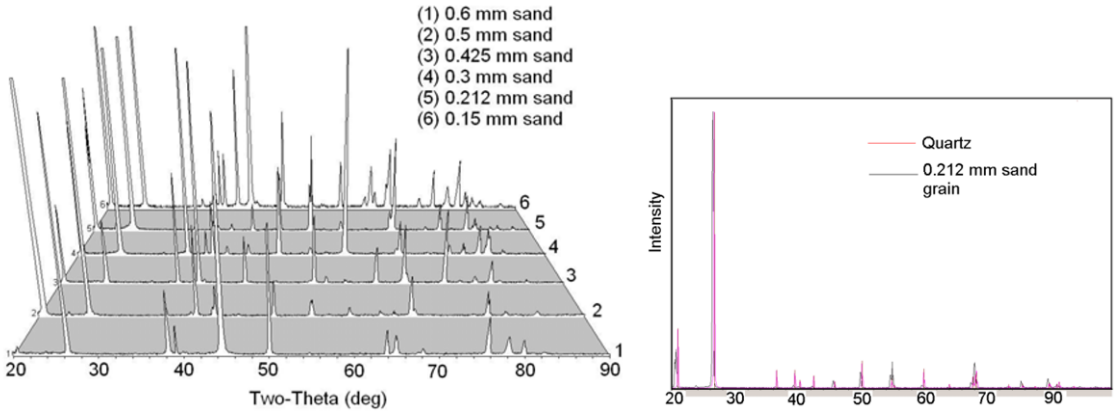

(a) (b)

Figure 2 (a) X-ray Diffraction pattern of Eglin sand grains.(b) X-ray Diffraction pattern comparison of quartz and 0.212 mm Eglin sand grains

The sand grains were embedded in an epoxy matrix and mounted in a sample holder. The samples were wet polished using an alumina abrasive powder (from Buehler Inc.) in water slurry. To obtain a smooth surface suitable for nanoindentation, the maximum abrasive size used in the final polishing was 50 nm. Figure 3 shows a polished sand surface with different grains oriented in different directions.

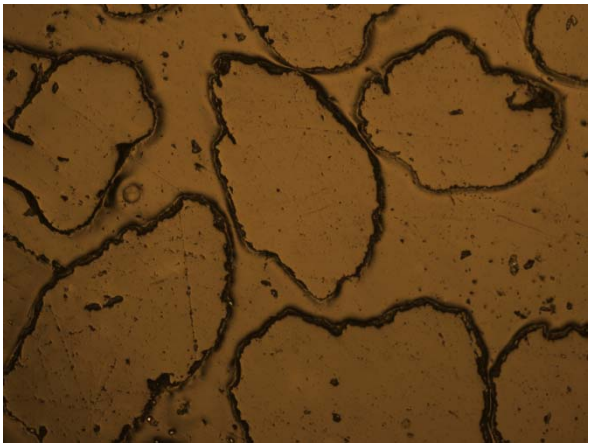

Figure 3. Magnified image of polished sand grains in an epoxy matrix

3. Nanoindentation tests in sand grains

An MTS Nano Indenter XP system was used for the nanoindentation measurements. This indenter can reach a maximum indentation depth of 500 μm and a maximum load of 500 mN. The displacement and load resolutions are 0.2 nm and 50 nN, respectively. Both Berkovich and cube-corner indenter tips, made of single crystal diamond, were used in this investigation. Nanoindentations were made on flat, polished sand grain surfaces under constant rate of loading.

Nanoindentations were carried out on 6 different sizes of sand grains with one test per grain. Young's modulus and hardness were obtained using the slope of the unloading curve and the values of load and contact area at maximum indentation depth. These were a direct output from the nanoindentation software. The distributions of modulus and hardness values are plotted in Figures 4 and 5, respectively. Six sizes of sand grains were embedded into the epoxy and polished separately. Nanoindentation measurements were conducted on these six samples. Table1 listed the Young's Modulus and Hardness of sand grains with different sizes from nanoindentation.

Using Weibull distribution function, we determined the median value (corresponding to P_{50} value) for Young's modulus of the six sizes of sand grains to be 97.44 GPa, 102.08 GPa, 108.9 GPa, 80.82 GPa, 77.48 GPa and 71.48 GPa respectively and hardness to be 13.21 GPa, 14.62 GPa, 15.55 GPa, 11.83 GPa, 10.92 GPa and 10.91 GPa respectively. Scattering in the data is attributed to different types of sand grains due primarily to variations in the material constituents, defect structure, and crystal orientations.

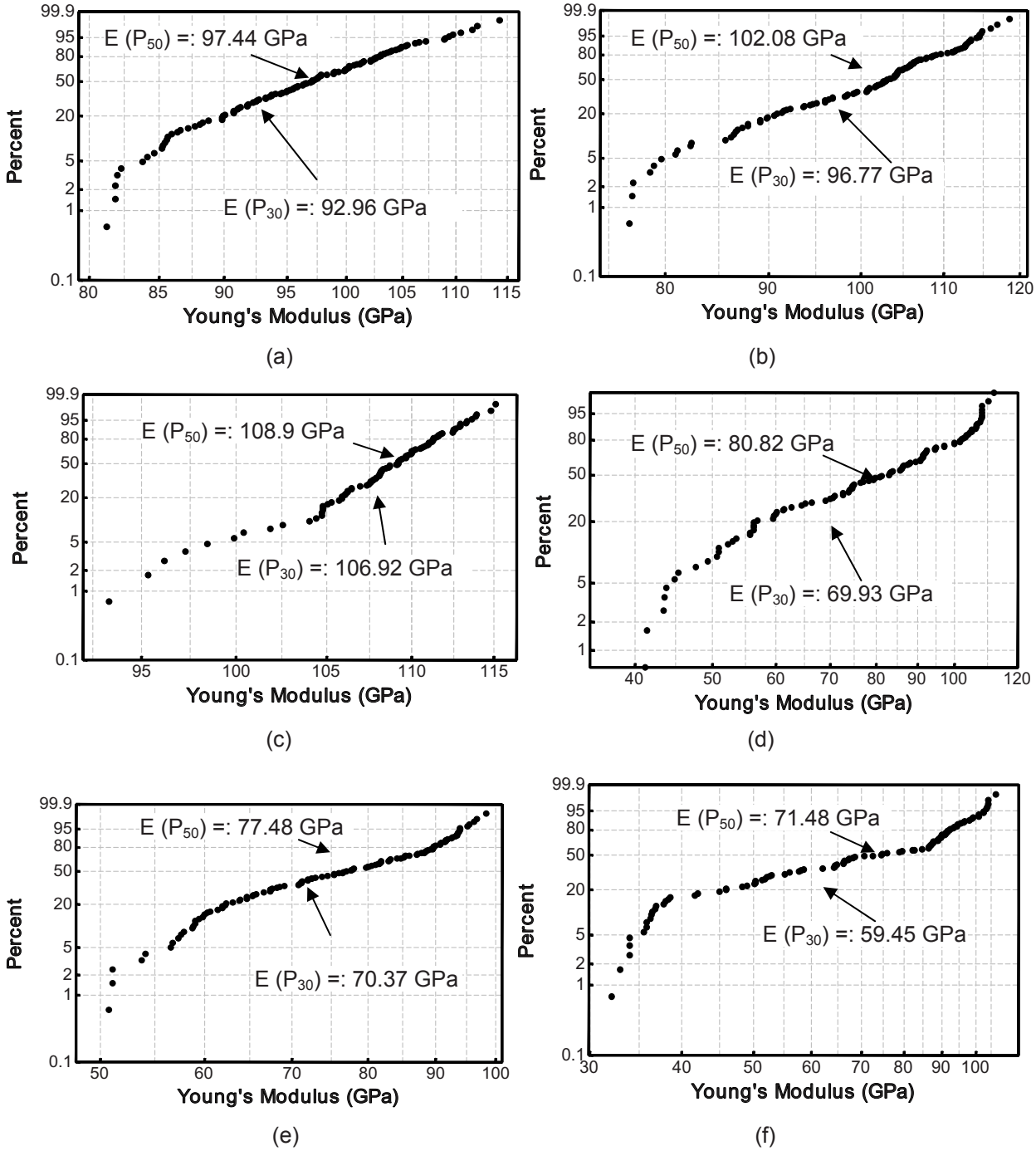

Figure 4(a): Weibull plot of Young's modulus from nanoindentations on 0.6 mm sand grains. (b): Weibull plot of Young's modulus of 0.5mm sand grains. (c): Weibull plot of Young's modulus of 0.425 mm sand grains. (d): Weibull plot of Young's modulus of 0.3mm sand grains. (e): Weibull plot of Young's modulus of 0.212 mm sand grains. (f): Weibull plot of Young's modulus of 0.15 mm sand grains.

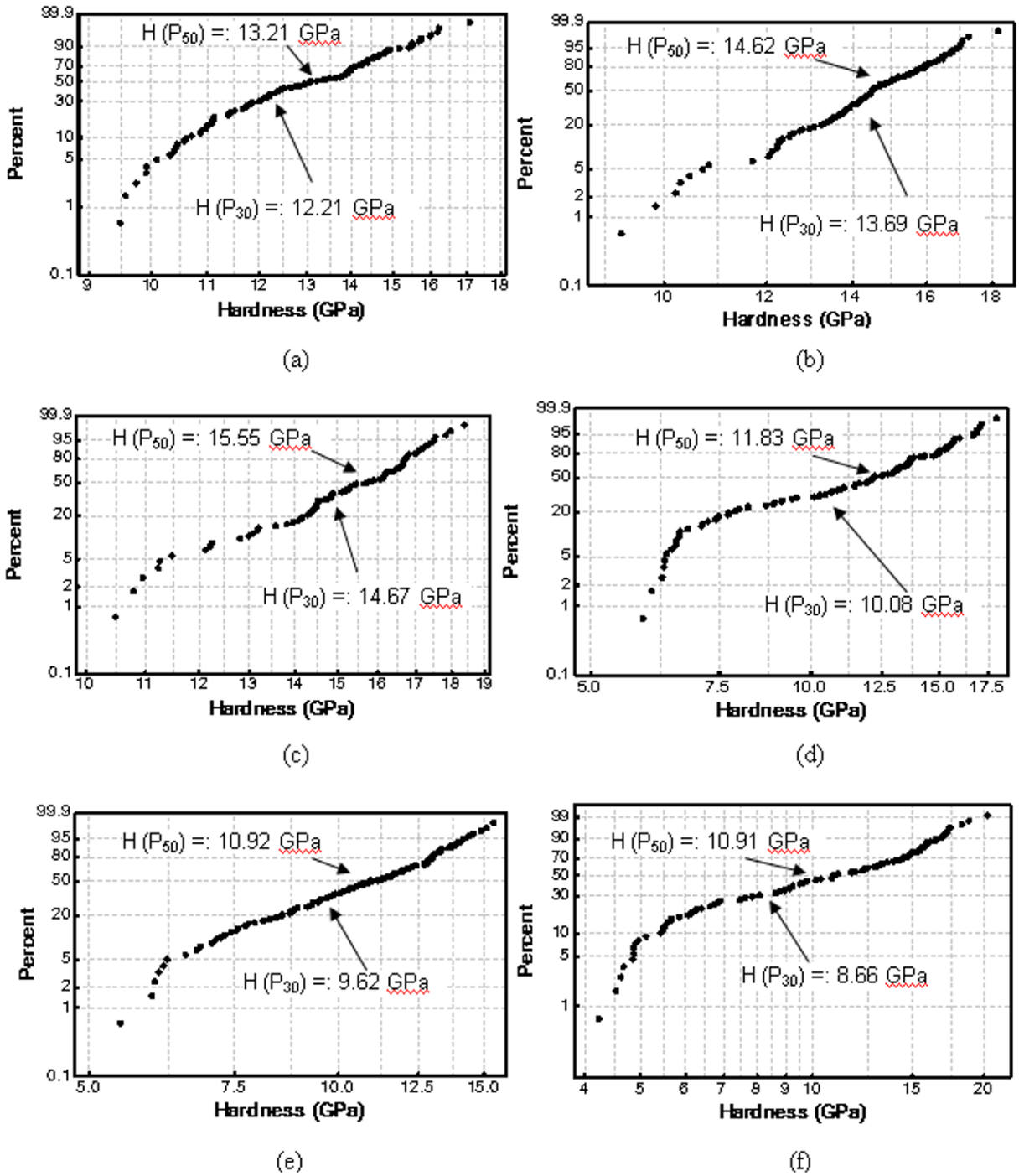

Figure 5(a): Weibull plot of hardness from nanoindentations on 0.6 mm sand grains. (b): Weibull plot of hardness of 0.5 mm sand grains. (c): Weibull plot of hardness of 0.425 mm sand grains. (d): Weibull plot of hardness of 0.3 mm sand grains. (e): Weibull plot of hardness of 0.212 mm sand grains. (f): Weibull plot of hardness of 0.15 mm sand grains.

It is well known that sand grains would generally behave in a brittle material under load. In order to estimate the fracture toughness, a formula derived by Pharr *et al.* [2] was used,

$$K_C = \alpha\left(\frac{E}{H}\right)^{0.5}\left(\frac{P}{c^{3/2}}\right) \qquad (1)$$

where α is an empirical constant which takes into account, the geometry of the indenter tip (for a cube-corner tip α = 0.032). Before proceeding with the nanoindentation on sand grains, a sample test was run on a standard fused silica sample (results not included here). The average value for fracture toughness obtained was 0.6 MPa-$m^{0.5}$ which is in reasonable agreement with the value reported for fused silica by Harding (1995) [3].

For sand, the values of the elastic modulus (E) and hardness (H) were obtained using the Berkovich nanoindenter tip prior to indenting with a cube-corner tip. Since we are interested in the ratio of E/H from the nanoindentation tests, we obtained an average value for the ratio as 8.5. In Eqn. (7), c is the crack length and can be determined from the surface scans obtained (two of the scans along with inverse images) are shown in Figure 6. Both 3D inverse images and 2D nanoindentation residual images are shown for details on the crack formation and fracture. It may be noted that due to slight errors in the alignment and inhomogeniety of the sand grain, it is rather difficult to induce three cracks with equal length. When there are differences between the crack lengths from the same indent, we have taken the average crack length for a particular indent. The histogram of the fracture toughness values obtained is shown in Figure 7(a) and the Weibull distribution in Figure 7(b). From the Weibull distribution, median value for the fracture toughness observed was 2.32 MPa-$m^{0.5}$ (range 1.3 to 4.0 MPa-$m^{0.5}$).

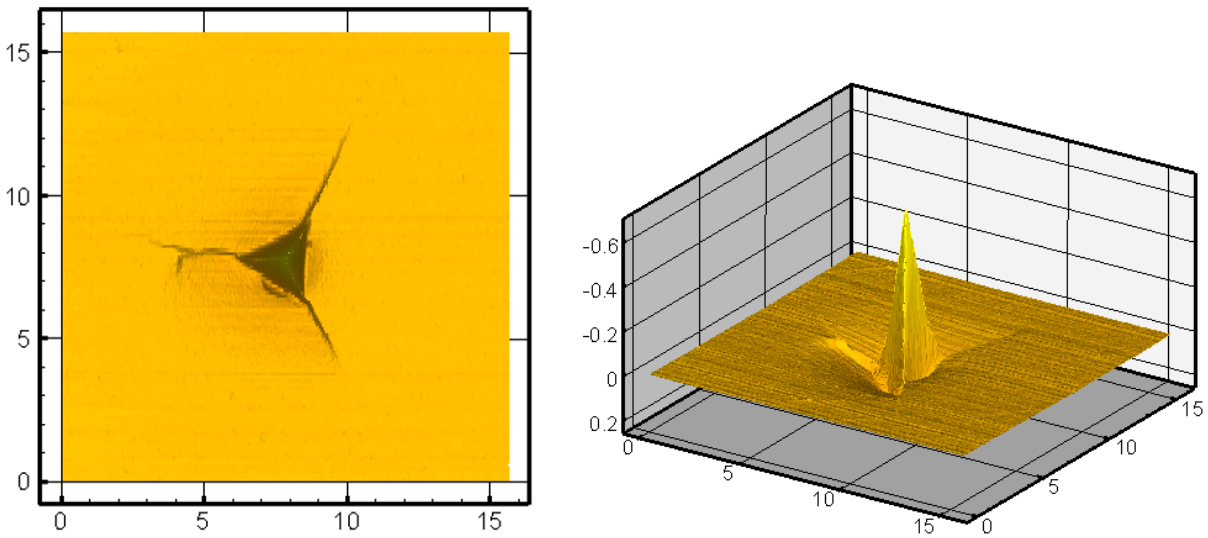

Figure 6: 2D residual surface profile and 3D inverse image showing cracks generated after nanoindentation using a cube corner tip at maximum load of 60 mN

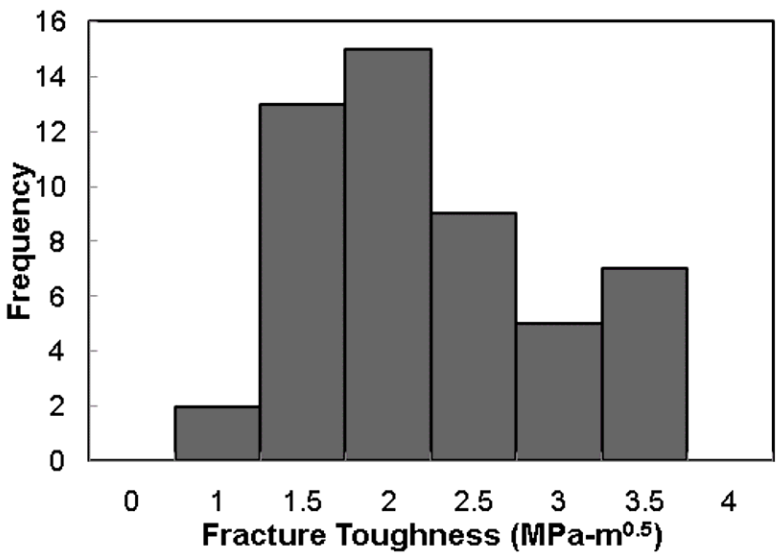

Figure 7(a): Distribution of fracture toughness for nanoindentations on different sand grains

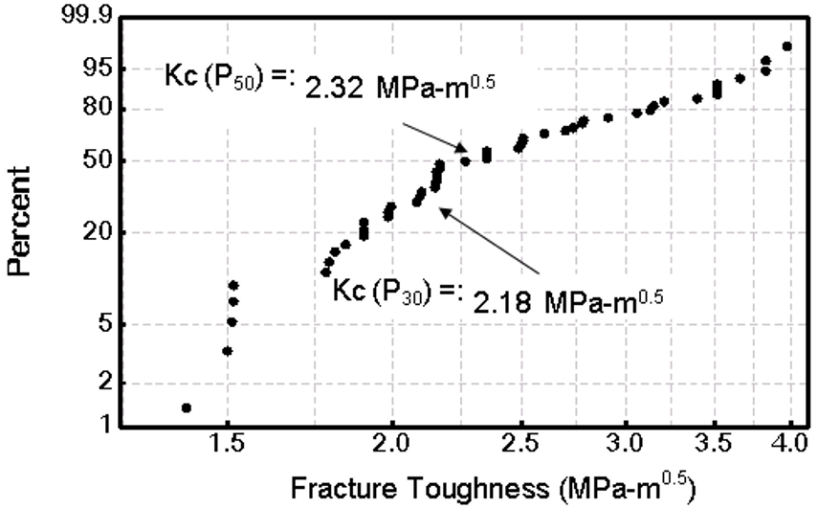

Figure 7(b): Weibull plot for fracture toughness from nanoindentations on different sand grains

4. Stress-strain response of Eglin sand grains

To determine the material properties parameters for granular sand material, nanoindentation experiment was modeled using FEM. To predict the elastic-plastic properties, von Mises yield criteria was used along with isotropic hardening to simulate the deformation characteristics of a sand grain. The plastic behavior under compression was assumed to satisfy the power law (Ramberg-Osgood) relationship between true stress and strain as

$\sigma_f = K \cdot \varepsilon^n$ for $\sigma_f \geq \sigma_y$ (2)

where *n* is the work hardening exponent, *K* is the reference stress value, and ε is the equivalent strain, $\varepsilon = \sqrt{\varepsilon_{ij}\varepsilon_{ij}} = \left(\varepsilon_y + \varepsilon_p\right)$, where ε_y is the yield strain and ε_p is the plastic strain. The von Mises equivalent stress is given as, $\sigma = \sqrt{\frac{3}{2}\sigma_{ij}\sigma_{ij}}$.

Within the linear elastic limit,

$\sigma = E\varepsilon$, for $\sigma \leq \sigma_y$ (3)

where *E* is the Young's modulus. In this work, ABAQUS V6.8-4 standard [4] was used to perform the calculations, assuming finite deformation characteristics. However, it is time consuming if the calculation only depends on fitting the simulation output with the experimental results since there are only a few parameters can be measured using nanoindentation, e.g. Young's modulus and parameter coupling effect might also increase the difficulty to obtain the reasonable values of material parameters, e.g. exponent of power law equation and yield stress. Therefore, a more efficient method should be concerned to overcome these problems. [5] reported a method to extract the stress-strain curve of single crystal materials by FEM simulation based the nanoindentation data. Their work is based on a relationship between hardness and flow stress first provided by Tabor [6] which is shown as the equation (4)

$H = C_\theta \cdot \sigma_f$ (4)

where C_θ is the "constraint factor" depending on the angle, θ, of indenter and flow stress is a characteristic value of plastic strain. The characteristic strain (ε_{char}) is able to be obtained for a given indenter angle. There have been several efforts to obtain the stress-strain curve by relating the hardness to stress and the indenter angle to characteristic strain. The power law equation of stress-strain relationship can be written as $K = \sigma_y(\sigma_y/E)^{-n}$ with the assumption linear elastic up to the yield strength. By combing equations (2), (4) and taking the logarithm, the hardness can be expressed as a function of *E*, σ_y, C_θ and ε_{char}, which is shown as equation (5),

$logH = n \cdot \log\left(\frac{E}{\sigma_y} \cdot \varepsilon_{char}\right) + \log\left(C_\theta \cdot \sigma_y\right)$ (5)

where the unknown values are only exponent *n* and yield stress σ_y for a given indenter angle. In this work, finite element simulation is used to solve the inverse problem to obtain the values of *n* and σ_y for the different size Eglin sand grains. Young's modulus, *E*, and hardness, *H* can be measured from nanoindenation experiments. We used

C_θ and ε_{char} values reported in [5] to calculate the input parameters n and σ_y for the FEM simulation. As mentioned previously, nanoindentation simulation results may be affected by parameters coupling, but based on equation (5) the two unknown parameters are dependable to each other, therefore, we just need to estimate one parameter and another value can be obtained using the equation automatically. In this case, only one parameter is estimated for the model's input and parameter coupling effect between yield stress and exponent has been considered.

The configuration for the FEM simulation of nanoindentation is shown in Figure 8. The Berkovich indenter was simulated based on its three sided pyramidal geometry. Because of the Berkovich indenter's axisymmetric geometry, only one sixth of the entire model was used in this simulation to concern the computational time. The displacement history from the experiment was given as input for the FE analysis. Poisson's ratio which was taken as 0.18 was used in this simulation and the values of Young's Modulus which is close to P50 value has been selected for different sizes. Also, the corresponding hardness values are substituted into equation (5) to calculate the unknown parameters. The different yield stress values were used to calculate the exponent value for the power law equation which is the input for the plastic behavior of sand. The output of the FE analysis was the resulting reaction force or load. This numerical load was plotted versus the displacement into the surface, to give load-displacement curve from the simulation. The mesh size selected was tested for convergence of the load-displacement curve. By changing the yield stress values for different size samples and compare the simulation output with experimental results until the reasonable agreement was reached, we can adjust the two unknown material parameters. The best-fit parameters were then used to determine the effective stress-strain relationship for the Eglin sand grain sample.

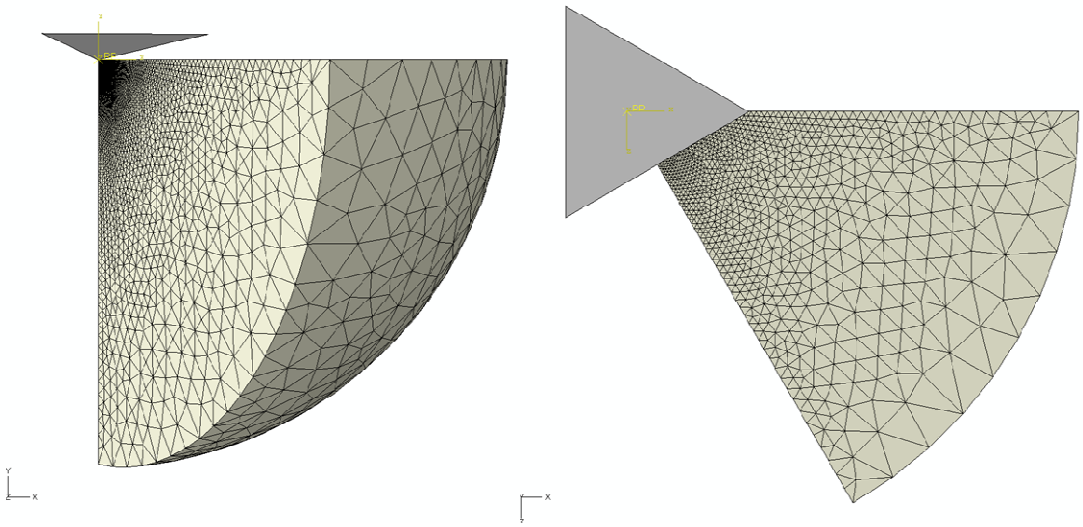

Figure 8 Side view and top view of axisymmetric Finite Element Analysis model for nanoindentation on 1/6 spherical sand grain using berkovich tip

It should be noted that the maximum strain up to which the stress-strain curve is valid, using this approach, is limited by the strain produced by the nanoindentation test [7]. No cracks were observed by examining the indent impressions (for the Berkovich indenter tip) obtained from Nanovision. Thus, the continuum plasticity material model was justified. As stated earlier, we used an inverse problem solving approach to determine the stress-strain relationship of sand at granular level by correlating the FEM simulated nanoindentation load-displacement data with the measured results. From the Figure 9, we can see the simulation results agree with the experimental results reasonably well. For all these six different sizes samples, and based on the representative experimental data P50, the values for yield stress and exponent of power law equation are about 2 ~ 3GPa and 0.99 ~ 1.15 respectively. These values with the measured Young's Modulus values can be used as the material parameters for the elastic-plastic constitutive model for Elgin sand grains.

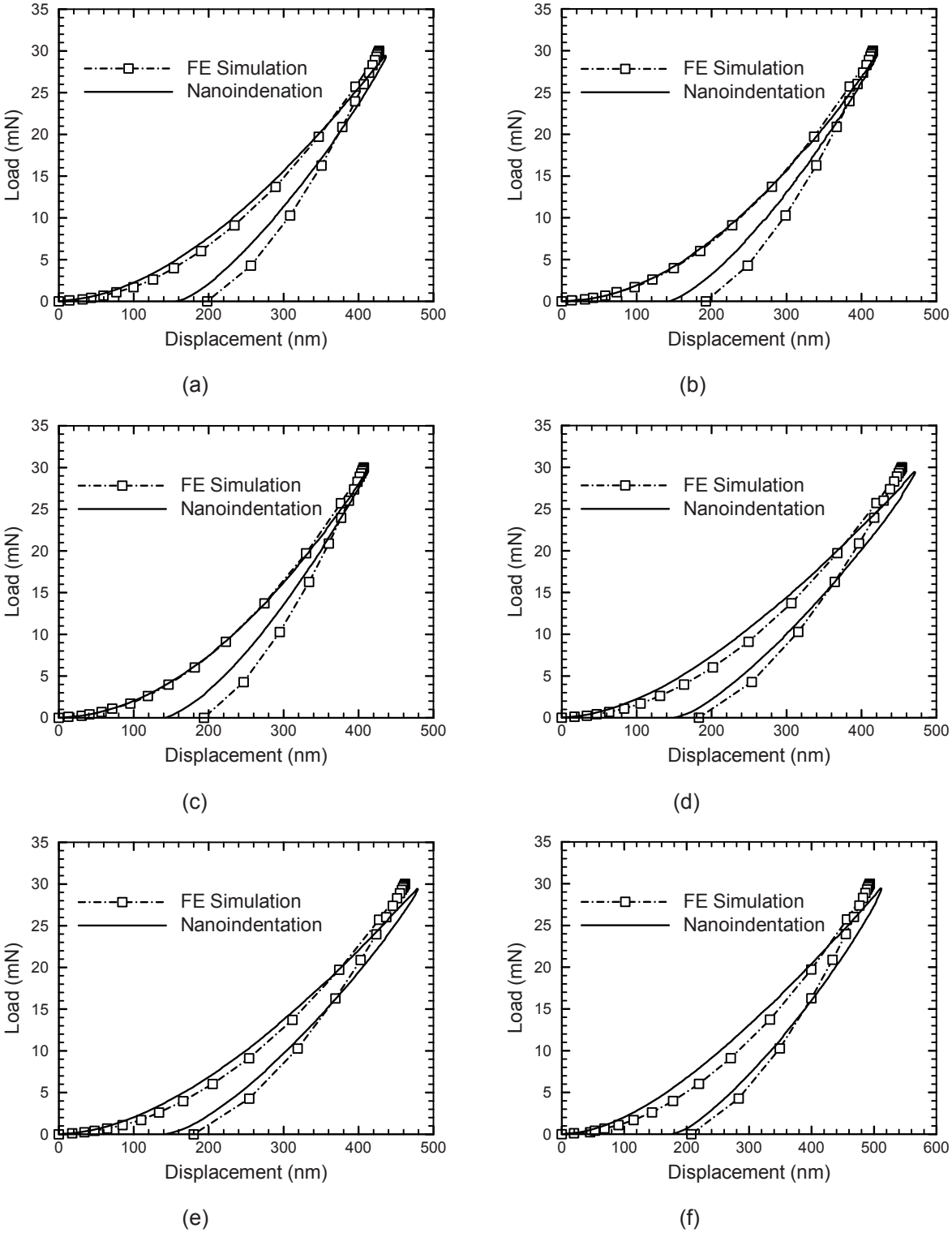

Figure 9 Comparison of experimental and simulation results for different size samples. (a): 0.6 mm sand grains. (b): 0.5mm sand grains. (c): 0.425 mm sand grains. (d): 0.3mm sand grains. (e): 0.212 mm sand grains. (f): 0.15 mm sand grains.

5. Conclusion

In order to assess the granular level mechanical behavior of sand, nanoindentation tests were conducted on individual sand grains to characterize their mechanical properties, namely, Young's elastic modulus, hardness, fracture toughness, and stress-strain relationship. Properties of six sizes of sand grains were concluded to obtain the size effect. As can be expected, a wide variation in the granular properties of sand was observed. Larger sand grains were found to have larger Young's modulus and hardness. The overall Young's modulus for the Eglin sand grains was found to be 90.38 GPa (range 33.4 to 119.8 GPa), hardness to be 12.84 GPa (range 4.2 to 20.3 GPa and fracture toughness to be 2.32 MPa-$m^{0.5}$ (range 1.3 to 4.0 MPa-$m^{0.5}$). Power-law was used to represent the homogenized and isotropic stress-strain behavior for sand at the granular level. However, the variation in the property value indicates that sand at granular level is very inhomogeneous and not isotropic due to different material constituents, defect structure, and crystal orientations. Need exists to establish the linkage between nanoindentation measured properties of sand grains with the observed macro properties for correct prediction of bulk behavior of sand. The data reported here can be used for mesoscale (granular) simulations of sand in which the individual sand grains would have different properties with the distributions obtained in this study.

Reference

[1] Oliver, W.C. and Pharr, G.M., 1992, "An Improved Technique for Determining Hardness and Elastic Modulus Using Load and Displacement Sensing Indentation Experiments," J. Mater. Res., 7, pp. 1564-1583.
[2] Pharr, G.M., Harding, D.S., and Oliver, W.C., 1993, "Measurement of fracture toughness in thin films and small volumes using nanoindentation method," Mechanical properties and deformation behavior of materials having ultra-fine microstructures, edited by M. Nastasi, D. M. Parkin, and H. Gleiter, Kluwer Academic Publishers, pp. 449-461.
[3] Harding, D.S., 1995, "Cracking during nanoindentation and its use in the measurement of fracture toughness," Materials Research Society symposia proceedings, 356 v.5, pp. 663-668.
[4] ABAQUS Documentation V 6.8, 2009.
[5] Shim, S., Jang, J., and Pharr, G. M., 2008, "Extraction of flow properties of single-crystal silicon carbide by nanoindentation and finite –element simulation," Acta Materialia, 56, pp. 3824-3832.
[6] Tabor, D., The hardness of metals, Oxford: Oxford University Press; 1951.
[7] Dao, M., Chollacoop, N., Van Vliet, K.J., Venkatesh, T.A., and Suresh, S., 2001, "Computational modeling of the forward and reverse problems in instrumented sharp indentation," Acta Mater., 49, pp. 3899-3918.